Key Points:
- We simulate the evolution of marine radiocarbon reservoir ages during the past 50,000 years
- Simulated low-latitude to midlatitude reservoir ages varied between 400 and 1200 ^{14}C years
- In high latitudes the simulated reservoir ages exceeded 2000 ^{14}C years

Marine radiocarbon reservoir age simulations for the past 50,000 years

M. Butzin[1] , **P. Köhler[1]** , **and G. Lohmann[1]**

[1]Alfred-Wegener-Institut Helmholtz-Zentrum für Polar-und Meeresforschung, Bremerhaven, Germany

Abstract Radiocarbon (^{14}C) dating calibration for the last glacial period largely relies on cross-dated marine ^{14}C records. However, marine reservoirs are isotopically depleted with respect to the atmosphere and therefore have to be corrected by the Marine Radiocarbon Ages of surface waters (MRAs), whose temporal variabilities are largely unknown. Here we present simulations of the spatial and temporal variability in MRAs using a three-dimensional ocean circulation model covering the past 50,000 years. Our simulations are compared to reconstructions of past surface ocean Δ^{14}C. Running the model with different climatic boundary conditions, we find that low-latitude to midlatitude MRAs have varied between 400 and 1200 ^{14}C years, with values of about 780 ^{14}C years at the Last Glacial Maximum. Reservoir ages exceeding 2000 ^{14}C years are simulated in the polar oceans. Our simulation results can be used as first-order approximation of the MRA variability in future radiocarbon calibration efforts.

1. Introduction

A critical problem in radiocarbon (^{14}C) dating is the variability of the atmospheric ^{14}C record. Within the most recent ^{14}C calibration effort, IntCal13 [*Reimer et al.*, 2013], however, underlying samples older than 13,900 calibrated years before present (13.9 kcal B.P.) are not based on the very precise, continuous tree ring record but on other archives—marine and lacustrine sediments, corals, and speleothems—which contain specific higher uncertainties [*Reimer et al.*, 2013]. Prior to this date, the ^{14}C calibration largely relies on marine records. However, marine ^{14}C reservoirs are systematically depleted with respect to the atmosphere because the primary source of ^{14}C is cosmogenic production in the upper atmosphere. Subsequent processes, such as isotopic air-sea exchange, oceanic mixing, and radioactive decay, all affect the ^{14}C concentrations in the different reservoirs. The isotopic depletion of surface water with respect to the atmosphere is frequently expressed in terms of the Marine Reservoir Age (MRA), i.e., the ^{14}C age of dissolved inorganic carbon in seawater with respect to the atmosphere. Nowadays, MRAs range from about 400 years in subtropical oceans to more than 1000 years in polar seas [*Key et al.*, 2004]. There is scattered evidence of regionally elevated MRAs in the past [for recent studies cf. *Austin et al.*, 2011; *Thornalley et al.*, 2011; *Bronk Ramsey et al.*, 2012; *Southon et al.*, 2012; *Stern and Lisiecki*, 2013; *de la Fuente et al.*, 2015; *Sarnthein et al.*, 2015; *Thornalley et al.*, 2015; *Balmer et al.*, 2016; *Sikes and Guilderson*, 2016; *Skinner et al.*, 2017], but overall, the global MRA history prior to the Holocene is poorly constrained. Therefore, MRA variability has been left aside in most radiocarbon calibration efforts [*Reimer et al.*, 2013]. Three-dimensional (3-D) ocean modeling may help to constrain past MRAs, but the long ^{14}C equilibration time of several thousands of years precludes model configurations with high resolution, and coarse resolution models have mostly focused on time slices or shorter periods [*Butzin et al.*, 2005; *Ritz et al.*, 2008; *Singarayer et al.*, 2008; *Butzin et al.*, 2012; *Galbraith et al.*, 2015], except for one long-term study [*Franke et al.*, 2008] not including the full glacial-interglacial variability of air-sea $^{14}CO_2$ fluxes.

Here we present a continuous, simulated history of spatiotemporally variable MRAs covering the past 50,000 years. The results were derived from 3-D ocean model calculations. After comparing our simulations with observations of past surface water concentration ratios (Δ^{14}C), we discuss the spatiotemporal evolution of past MRAs and potential implications.

2. Methods

We apply an enhanced version of the Hamburg LSG ocean general circulation model ([*Maier-Reimer et al.*, 1993], subsequent enhancements include a bottom-boundary layer [*Lohmann*, 1998] and improved advection and mixing schemes [*Schäfer-Neth and Paul*, 2001; *Prange et al.*, 2003; *Butzin et al.*, 2005]). The

spatial resolution is 3.5° in horizontal direction including 22 unevenly spaced levels in the vertical dimension. The model is forced with monthly fields of wind stress, surface air temperature, and freshwater flux. These forcing fields of the ocean model were obtained from previous climate simulations in which the atmosphere general circulation model ECHAM3/T42 was forced with reconstructed values of insolation, greenhouse gases, ice sheets, sea-ice cover, and sea surface temperatures [*Lohmann and Lorenz*, 2000; *Prange et al.*, 2004]. The temperature boundary condition is formulated as a scale dependent restoring mimicking an atmospheric energy balance model [*Prange et al.*, 2003].

To capture the range of climate variability during the past 50,000 years, we consider three background scenarios which are discussed in detail elsewhere [*Butzin et al.*, 2005; *Hesse et al.*, 2011; *Butzin et al.*, 2012]. To summarize, one scenario (PD) employs present-day climate background to represent the Holocene and interstadials. The other scenarios utilize boundary conditions derived for the Last Glacial Maximum (LGM). Glacial scenario GS is based on the Glacial Atlantic Ocean Mapping 2000 reconstruction [*Sarnthein et al.*, 2003, and references therein; *Paul and Schäfer-Neth*, 2003]. The second glacial climate scenario (CS) is based on the Climate: Long-Range Investigation, Mapping, and Prediction reconstruction [*CLIMAP Project Members*, 1981] with additional tropical cooling [*Lohmann and Lorenz*, 2000]. In both glacial scenarios the freshwater balance in the Southern Ocean has been modified to mimic enhanced sea ice export, leading to intensified formation of deep and bottom waters in the Southern Ocean while deep water formation in the North Atlantic shoals and weakens [*Butzin et al.*, 2005]. In scenario GS the meridional overturning circulation (MOC) decreases by about 30% compared to PD. Scenario CS features MOC weakening by 60% and thermohaline properties characteristic of Heinrich stadials [*Sarnthein et al.*, 1994].

Radiocarbon is simulated as $\Delta^{14}C$ (i.e., the normalized $^{14}C/^{12}C$ ratio in seawater corrected for isotopic fractionation) similar to *Toggweiler et al.* [1989]. We do not prescribe temporal changes in ^{14}C production rates, as done in other approaches [e.g., *Köhler et al.*, 2006], but derive marine $\Delta^{14}C$ directly from atmospheric $\Delta^{14}C$ [*Reimer et al.*, 2013]. For this effort we calculate air-sea exchange fluxes of $\Delta^{14}C$ following *Sweeney et al.* [2007], considering wind speed data from our atmospheric forcing fields, transient partial pressures of atmospheric carbon dioxide (pCO$_2$; based on mixing ratios by *Bereiter et al.* [2015]), and persistent concentrations of dissolved inorganic carbon in the mixed layer by *Hesse et al.* [2011]. Marine reservoir ages (in ^{14}C years) are calculated a posteriori as

$$MRA = \lambda^{-1} \ln \left[\left(0.001\ \Delta^{14}C_{atm} + 1 \right) / \left(0.001\ \Delta^{14}C_{mar} + 1 \right) \right] \quad (1)$$

where $\Delta^{14}C_{atm}$ and $\Delta^{14}C_{mar}$ are the $\Delta^{14}C$ values in atmosphere and ocean, and λ^{-1} = 8033 years is the conventional decay constant of ^{14}C. Our simulations agree with prebomb and glacial observations of marine $\Delta^{14}C$ [cf. *Butzin et al.*, 2005; *Butzin et al.*, 2012]. Moreover, *Hesse et al.* [2011] have shown that the circulation fields resulting from forcing scenarios GS and CS are also in line with stable carbon isotope ($\delta^{13}C$) measurements in the glacial Atlantic.

Our model runs start from quasi steady state conditions typical for 50 kcal B.P., which were obtained in spin-up integrations (over 20,000 years) using fixed atmospheric background values of $\Delta^{14}C$ = 300‰ [*Reimer et al.*, 2013] and pCO$_2$ = 200 μatm [*Bereiter et al.*, 2015]. The transient simulations are run forward in time forced with atmospheric $\Delta^{14}C$ provided by IntCal13 [*Reimer et al.*, 2013] and pCO$_2$ according to ice core reconstructions [*Bereiter et al.*, 2015] (time series are shown in the supporting information, Figure S1). For the period 50–11.5 kcal B.P. we consider all three scenarios: PD, GS, and CS. For times more recent than 11.5 kcal B.P. we only consider model results for scenario PD.

3. Results and Discussion

3.1. Comparison With Near-Surface $\Delta^{14}C$ Paleorecords

We evaluate our model with near-surface $\Delta^{14}C$ paleorecords from six locations in the Atlantic, Indian, and Pacific Oceans. Our simulations match the long-term decline of $\Delta^{14}C$ seen in all paleorecords since about 25 kcal B.P. (Figure 1). Moreover, our model captures the $\Delta^{14}C$ excursion recorded at some locations during the Younger Dryas at around 12 kcal B.P. (Figures 1a, 1b, 1c, and 1e). The agreement between simulations and reconstructions deteriorates prior to about 30 kcal B.P. Our results are within the uncertainty range of the Iberian Margin and Pakistan Margin records, but our simulations are unable to reproduce peak values reconstructed in other marginal seas or tropical lagoons. This is particularly obvious in the Cariaco Basin, where the
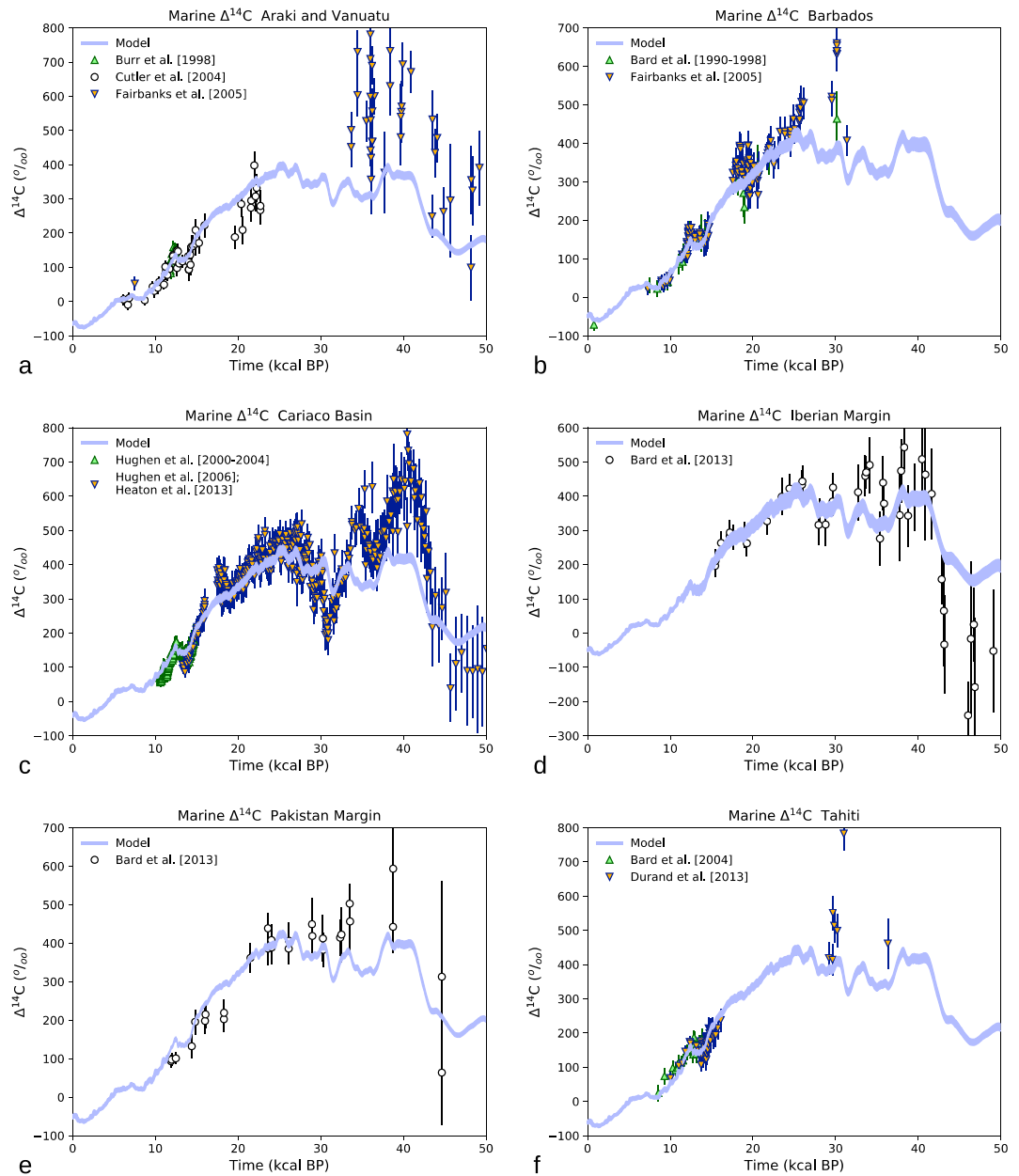
Figure 1. Simulation results and reconstructions of marine Δ^{14}C at various locations, (a) Araki and Vanuatu (15.6°S, 167.0°E) [*Burr et al.*, 1998; *Cutler et al.*, 2004; *Fairbanks et al.*, 2005], (b) Barbados (13.1°N, 59.3°W) [*Bard et al.*, 1990, 1998; *Fairbanks et al.*, 2005], (c) Cariaco Basin (10.7°N, 65.2°W) [*Hughen et al.*, 2000; *K. Hughen et al.*, 2004; *K. A. Hughen et al.*, 2004; *Hughen et al.*, 2006; *Heaton et al.*, 2013], (d) Iberian Margin (37.8°N, 10.2°E) [*Bard et al.*, 2013], (e) Pakistan Margin (24.8°N, 64.0°E) [*Bard et al.*, 2013], (f) Tahiti (17.5°S, 149.6°W) [*Bard et al.*, 2004; *Durand et al.*, 2013]. Simulation results span upper and lower bounds and are evaluated at the grid points nearest to the reconstructions at the first model layer (depth range 0–50 m). Error bars of the data points indicate the reconstruction uncertainty (1σ). Reconstructions were obtained from the IntCal13 database (http://calib.org/intcal13/, accessed on 9 September 2016).

amplitude of Δ^{14}C reconstructions between 30 and 40 kcal B.P. is even larger than the amplitude of the IntCal13 time series of atmospheric Δ^{14}C used to force our simulations. The temporal variability of the Cariaco Basin record will be discussed below.

### 3.2. Large-Scale Evolution of Marine Reservoir Ages

Marine reservoir ages are frequently reconstructed from planktonic foraminifera, typically dwelling in the upper 300 m of the oceans with species-specific preferences in habitat depth. To explore the effect of
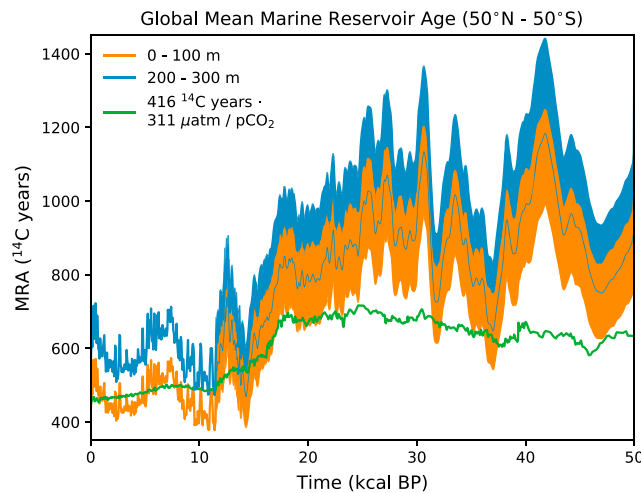
Figure 2. Simulated history of the mean marine reservoir age (averaged between 50°N and 50°S), shown are upper and lower bounds spanned by the ocean climate scenarios for the depth ranges 0–100 m and 200–300 m. The thin blue line marks the lower bound of values for 200–300 m. The green curve illustrates the effect of pCO$_2$ variations, scaling the mean MRA simulated for year 0 cal B.P. (about 416 ^{14}C years between 0 and 100 m, using pCO$_2$ = 311 μatm) with past pCO$_2$ values based on reconstructions [*Bereiter et al.*, 2015].

habitat depth in MRA reconstructions, we evaluate our simulation results for the water depths 0–100 m and 200–300 m. Considering the upper 100 m and taking the average between 50°N and 50°S, we find that the mean MRA has varied between about 400 and 1200 ^{14}C years (Figure 2). During the last 11.5 kyr the simulated mean MRA has varied between 380 and 570 ^{14}C years. Looking further back in time, our simulations display a global MRA excursion to 780 ^{14}C years during the Younger Dryas, preceded by a pronounced decline during the last glacial termination. According to our simulations, the mean MRA was about 780 ^{14}C years at the LGM. Prior to about 25 kcal B.P., our simulations show MRA oscillations between 540 and 1250 ^{14}C years with peak values around 42 kcal B.P. The ampli-

tude of those oscillations is much larger than the uncertainty range introduced by the various ocean climate scenarios, which is about ±100 ^{14}C years. The mean MRA shows similar temporal variability at 200–300 m water depth, exhibiting values typically elevated by 130 ^{14}C years when compared to the upper 100 m.
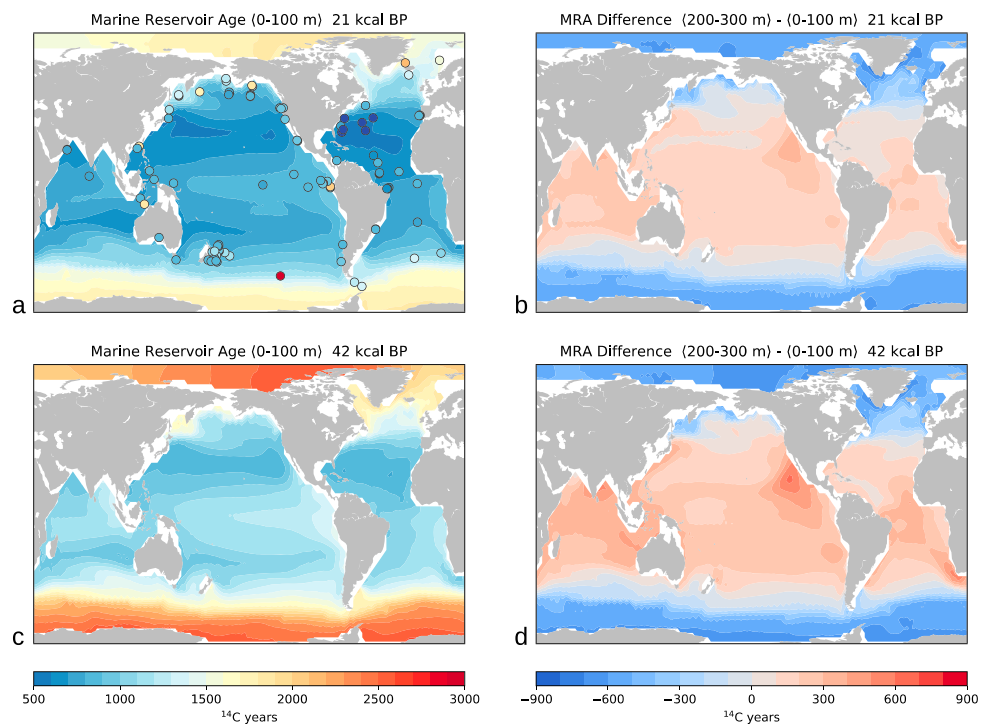
Figure 3. Maps of simulated marine reservoir ages at two times, (a) 21 kcal B.P. (around the LGM), depth range 0–100 m; filled circles are values adopted by *Skinner et al.* [2017]; (b) 21 kcal B.P., MRA difference between the depth ranges 200–300 m and 0–100 m; (c) 42 kcal B.P. (around the Laschamp event [*Laj et al.*, 2014]), depth range 0–100 m; and (d) 42 kcal B.P., MRA difference between 200–300 m and 0–100 m. See *Butzin et al.* [2012] to compare with preindustrial values.
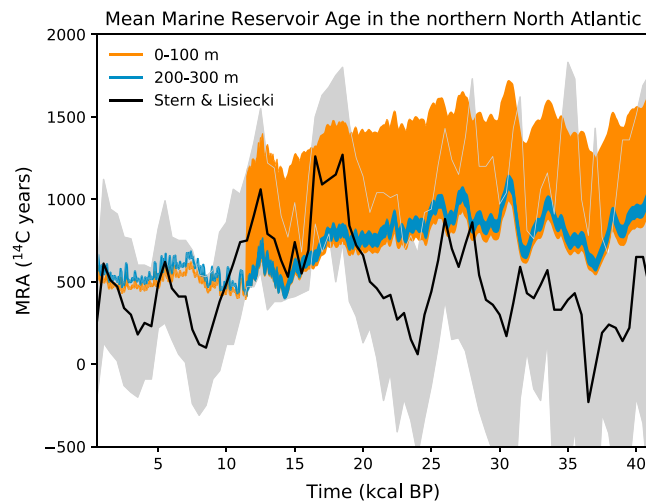
Figure 4. History of regionally averaged marine reservoir ages in the high-latitude North Atlantic. The gray envelope marks 95% confidence intervals of the reconstruction by *Stern and Lisiecki* [2013]. Our simulation results are averages over the sampling area of open-ocean sediment cores (about 40°N–65°N, 10°W–50°W) for two different depth ranges (0–100 m and 200–300 m).

At all times and at both depths, our simulations display the lowest MRAs in the subtropics and the highest MRAs in polar regions where sea-ice inhibits the uptake of $^{14}CO_2$ (Figures 3a and 3c). The inhibition through sea ice decreases in the subsurface layer where the isotopic depletion is replenished through lateral mixing (Figures 3b and 3d). This implies that the meridional MRA variation weakens with depth from about 1200 ^{14}C years to 500 ^{14}C years at the LGM and from about 1800 ^{14}C years to 900 ^{14}C years at 42 kcal B.P. (not shown). Our model results for the LGM are in line with MRA estimates adopted by *Skinner et al.* [2017] (Figure 3a).

Carbon-isotopic air-sea exchange rates and hence MRAs vary with the partial pressure of atmospheric CO_2. Scaling the average modern MRA (416 ^{14}C years at year 0 B.P. according to model run PD averaged between 50°N and 50°S and over the upper 100 m) with the CO_2 history, we estimate that glacial CO_2 lowering alone could have increased global mean MRAs to 600–700 ^{14}C years (Figure 2). The variability of the CO_2 paleorecord is too small to explain the millenial-scale MRA fluctuations of several hundreds of ^{14}C years prior to the LGM. Those variations reflect time lags between atmospheric ^{14}C forcing and ^{14}C exchange with the deep sea. The input time series of atmospheric $\Delta^{14}C$ features rapid excursions around 41, 33, 31, and 27 kcal B.P. (not shown), which can be attributed to ^{14}C production peaks [*Köhler et al.*, 2006; *Hain et al.*, 2014]. Cosmogenic ^{14}C production spikes may induce MRA shifts without any changes in air-sea $^{14}CO_2$ exchange or oceanic overturning, because the response of the interior ocean to rapid atmospheric ^{14}C variations is slow. To some extent, this memory effect depends on the vertical mixing strength. As mixing parametrizations vary between ocean general circulation models, it would be interesting to see if other 3-D ocean models could reproduce our pre-LGM MRA oscillations which are poorly constrained through the few available open ocean ^{14}C records.

There is no global reconstruction of pelagic MRAs prior to 25 kcal B.P., but there is an area-covering reconstruction of MRAs in the northern North Atlantic extending to 41 kcal B.P. by *Stern and Lisiecki* [2013]. Averaged over their sampling area (about 40°N–65°N, 10°W–50°W) our simulation results show considerably less temporal variability than reconstructed, and our simulated MRAs are at the upper range of reconstructed values for times prior to the LGM (Figure 4). The reconstruction by *Stern and Lisiecki* [2013] involves invariant MRAs at low latitudes, disregarding the influence of past pCO_2 variations. We presume that this factor could incline their results toward our findings. The muted temporal variability of our simulation results reflects the smoothness of the atmospheric $\Delta^{14}C$ input curve. To account for unquantified errors, this curve was constructed in a way largely removing the centennial- and millennial-scale fluctuations seen in many individual ^{14}C records [*Reimer et al.*, 2013]. However, as the observational uncertainties prior to the tree ring period can become too large to separate real ^{14}C variations from random fluctuations, it is not clear to what extent the differences in temporal variability can be attributed to uncertainties of the input curve.
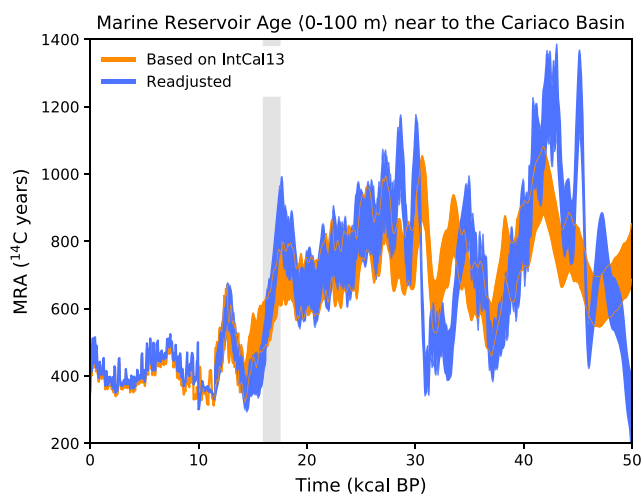
3.3. Revisiting the Cariaco Basin ^{14}C Record

The longest continuous marine ^{14}C record has been sampled in the Cariaco Basin (10.7°N, 65.2°W [*Hughen et al.*, 2000; *K. Hughen et al.*, 2004; *K. A. Hughen et al.*, 2004; *Hughen et al.*, 2006]). The data have contributed to ^{14}C calibrations such as IntCal13 assuming an invariant MRA of 430 ^{14}C years. However, analyses of a ^{14}C chronology from Lake Suigetsu point to MRAs of 0–1000 ^{14}C years in the Caribbean for 14–24 kcal B.P. [*Bronk*

Figure 5. Comparison of marine reservoir ages simulated in the Caribbean Sea near to the Cariaco Basin. The orange envelope shows the MRA history using atmospheric $\Delta^{14}C$ input values according to IntCal13, originally assuming for the local reservoir an invariant value of 430 ^{14}C years. The blue envelope is the simulated reservoir age history obtained when marine and the atmospheric input time series of $\Delta^{14}C$ are iteratively corrected ("readjusted") for variable reservoir ages. The gray box indicates the period 16.0–17.5 kcal B.P. See the main text and *Butzin et al.* [2012] for further explanation.

Ramsey et al., 2012]. Comparing our simulations at the grid point nearest to the Cariaco Basin, our model displays MRA variations between 300 and 1100 ^{14}C years prior to the Holocene (Figure 5). The use of a constant global MRA in IntCal13 could be corrected by an iterative calculation scheme [*Butzin et al.*, 2012]. The idea involves back and forth simulations of $\Delta^{14}C$ in atmosphere and ocean until simulated seawater $\Delta^{14}C$ values fit to reconstructions. The simulations converge to the reconstructions after three iterations. Applying this approach to the most recent version of the Cariaco Basin ^{14}C record (*Hughen et al.* [2006] with calendar age model revised by *Heaton et al.* [2013]), the amplitude of near-site MRA variations increases to 300–1400 ^{14}C years (Figure 5). The differences of these readjusted simulations to our original (not adjusted) simulation results are small until 27 kcal B.P. except for Heinrich Stadial 1 (HS1). Note that the Cariaco Basin record during 16.0–17.5 kcal B.P. was excluded from the IntCal13 data set because of potential local reservoir age changes [*Reimer et al.*, 2013].

Water exchange between the Cariaco Basin and the Atlantic is restricted by a shallow sill with a depth of about 140 m nowadays, and less than 30 m during the LGM [*Peterson et al.*, 1991]. Therefore, the Cariaco Basin should be decoupled from the global deepwater ^{14}C reservoir and its memory effects discussed above. As the small-scale bathymetry of the Cariaco Basin is not resolved in our model due to its coarse resolution, the MRA fluctuations seen in our simulations may be biased through too much mixing with North Atlantic Deep Water or Glacial North Atlantic Intermediate Water.

4. Conclusions

Our simulation results are broadly in line with available marine ^{14}C reconstructions since before the LGM. This agreement suggests that our simulations are able to capture the general evolution of past MRAs, at least for the past 25,000 years. Moreover, our model calculations reveal considerable spatial and temporal MRA variations during the past 50,000 years. The evolution of open-ocean MRAs may have been influenced by leads and lags between atmospheric ^{14}C production and radioactive decay in the interior of the oceans. To some extent, such memory effects reflect the intensity of vertical mixing, something that is still debated in (paleo)oceanographic research (see *Jayne et al.* [2004] for an overview). This issue deserves further efforts combining simulations and reconstructions, all the more, as uncertainties in reconstructions are large for times prior to about 30 kcal B.P. The simulated open-ocean MRA variability is poorly constrained through reconstructions. Surface water ^{14}C paleorecords typically originate from continental margins, marginal seas, or tropical lagoons which are not properly resolved by coarse-resolution ocean models and may result in regional model biases. The resolution problem could be overcome by the next generation of ^{14}C-equipped ocean circulation models, either through nesting approaches or by means of global multiresolution models with unstructured meshes [e.g., *Danilov et al.*, 2017].

References

Austin, W. E. N., R. J. Telford, U. S. Ninnemann, L. Brown, L. J. Wilson, D. P. Small, and C. L. Bryant (2011), North Atlantic reservoir ages linked to high Younger Dryas atmospheric radiocarbon concentrations, *Rapid Clim. Change Lessons Recent Geol. Past*, 79(3–4), 226–233, doi:10.1016/j.gloplacha.2011.06.011.

Balmer, S., M. Sarnthein, M. Mudelsee, and P. M. Grootes (2016), Refined modeling and ^{14}C plateau tuning reveal consistent patterns of glacial and deglacial 14C reservoir ages of surface waters in low-latitude Atlantic, *Paleoceanography*, *31*, 1030–1040, doi:10.1002/2016PA002953.

Bard, E., B. Hamelin, R. G. Fairbanks, and A. Zindler (1990), Calibration of the ^{14}C timescale over the past 30,000 years using mass spectrometric U-Th ages from Barbados corals, *Nature*, *345*(6274), 405–410, doi:10.1038/345405a0.

Bard, E., M. Arnold, B. Hamelin, N. Tisnerat-Laborde, and G. Cabioch (1998), Radiocarbon calibration by means of mass spectrometric ^{230}Th/^{234}U and ^{14}C ages of corals, *An updated data base including samples from Barbados, Mururoa and Tahiti, Radiocarbon*, *40*, 1085–1092, doi:10.1017/S0033822200019135.

Bard, E., G. Menot-Combes, and F. Rostek (2004), Present status of radiocarbon calibration and comparison records based on Polynesian corals and Iberian Margin sediments, *Radiocarbon*, *46*, 1189–1202, doi:10.1017/S0033822200033087.

Bard, E., G. Ménot, F. Rostek, L. Licari, P. Böning, R. L. Edwards, H. Cheng, Y. Wang, and T. J. Heaton (2013), Radiocarbon calibration/comparison records based on marine sediments from the Pakistan and Iberian Margins, *Radiocarbon*, *55*, 1999–2019, doi:10.2458/azu_js_rc.55.17114.

Bereiter, B., S. Eggleston, J. Schmitt, C. Nehrbass-Ahles, T. F. Stocker, H. Fischer, S. Kipfstuhl, and J. Chappellaz (2015), Revision of the EPICA Dome C CO_2 record from 800 to 600 kyr before present, *Geophys. Res. Lett.*, *42*, 542–549, doi:10.1002/2014GL061957.

Bronk Ramsey, C., et al. (2012), A complete terrestrial radiocarbon record for 11.2 to 52.8 kyr B.P, *Science*, *338*, 370–374, doi:10.1126/science.1226660.

Burr, G. S., J. W. Beck, F. W. Taylor, J. Recy, R. L. Edwards, G. Cabioch, T. Correge, D. J. Donahue, and J. M. O'Malley (1998), A high-resolution radiocarbon calibration between 11,700 and 12,400 calendar years BP derived from ^{230}Th ages of corals from Espiritu Santo Island, Vanuatu., *Radiocarbon*, *40*, 1093–1105, doi:10.1017/S0033822200019147.

Butzin, M., M. Prange, and G. Lohmann (2005), Radiocarbon simulations for the glacial ocean: The effects of wind stress, Southern Ocean sea ice and Heinrich events, *Earth Planet. Sci. Lett.*, *235*(1–2), 45–61, doi:10.1016/j.epsl.2005.03.003.

Butzin, M., M. Prange, and G. Lohmann (2012), Readjustment of glacial radiocarbon chronologies by self-consistent three-dimensional ocean circulation modeling, *Earth Planet. Sci. Lett.*, *317–318*, 177–184, doi:10.1016/j.epsl.2011.11.046.

CLIMAP Project Members (1981), Seasonal reconstructions of the Earth's surface at the Last Glacial Maximum, Geol. Soc. Am. Map Chart Ser., Geol. Soc. of Am., Boulder, Colo.

Cutler, K. B., S. C. Gray, G. S. Burr, R. L. Edwards, F. W. Taylor, G. Cabioch, J. W. Beck, H. Cheng, and J. Moore (2004), Radiocarbon calibration to 50 kyr BP with paired ^{14}C and ^{230}Th dating of corals from Vanuatu and Papua New Guinea, *Radiocarbon*, *46*, 1127–1160, doi:10.1017/S0033822200033063.

Danilov, S., D. Sidorenko, Q. Wang, and T. Jung (2017), The Finite-volumE Sea ice–Ocean Model (FESOM2), *Geosci. Model Dev.*, *10*(2), 765–789, doi:10.5194/gmd-10-765-2017.

de la Fuente, M., L. Skinner, E. Calvo, C. Pelejero and I Cacho (2015), Increased reservoir ages and poorly ventilated deep waters inferred in the glacial Eastern Equatorial Pacific, *Nat. Commun.*, *6*, 7420, doi:10.1038/ncomms8420.

Durand, N., P. Deschamps, E. Bard, B. Hamelin, G. Camoin, A. L. Thomas, G. M. Henderson, Y. Yokoyama, and H. Matsuzaki (2013), Comparison of ^{14}C and U-Th Ages in Corals from IODP #310 Cores Offshore Tahiti, *Radiocarbon*, *55*, 1947–1974, doi:10.2458/azu_js_rc.v55i2.16134.

Fairbanks, R. G., R. A. Mortlock, T.-C. Chiu, L. Cao, A. Kaplan, T. P. Guilderson, T. W. Fairbanks, A. L. Bloom, P. M. Grootes, and M.-J. Nadeau (2005), Radiocarbon calibration curve spanning 0 to 50,000 years BP based on paired ^{230}Th/^{234}U/^{238}U and ^{14}C dates on pristine corals, *Quat. Sci. Rev.*, *24*(16–17), 1781–1796, doi:10.1016/j.quascirev.2005.04.007.

Franke, J., A. Paul, and M. Schulz (2008), Modeling variations of marine reservoir ages during the last 45 000 years, *Clim. Past*, *4*, 125–136, doi:10.5194/cp-4-125-2008.

Galbraith, E. D., E. Y. Kwon, D. Bianchi, M. P. Hain, and J. L. Sarmiento (2015), The impact of atmospheric pCO$_2$ on carbon isotope ratios of the atmosphere and ocean, *Global Biogeochem. Cycles*, *29*, 307–324, doi:10.1002/2014GB004929.

Hain, M. P., D. M. Sigman, and G. H. Haug (2014), Distinct roles of the Southern Ocean and North Atlantic in the deglacial atmospheric radiocarbon decline, *Earth Planet. Sci. Lett.*, *394*, 198–208, doi:10.1016/j.epsl.2014.03.020.

Heaton, T. J., E. Bard, and K. A. Hughen (2013), Elastic tie-pointing—Transferring chronologies between records via a Gaussian process, *Radiocarbon*, *55*(04), 1975–1997, doi:10.2458/azu_js_rc.55.17777.

Hesse, T., M. Butzin, T. Bickert, and G. Lohmann (2011), A model-data comparison of δ^{13}C in the glacial Atlantic Ocean, *Paleoceanography*, *26*, PA3220, doi:10.1029/2010PA002085.

Hughen, K., S. Lehman, J. Southon, J. Overpeck, O. Marchal, C. Herring, and J. Turnbull (2004), ^{14}C activity and global carbon cycle changes over the past 50,000 years, *Science*, *303*(5655), 202, doi:10.1126/science.1090300.

Hughen, K., J. Southon, S. Lehman, C. Bertrand, and J. Turnbull (2006), Marine-derived ^{14}C calibration and activity record for the past 50,000 years updated from the Cariaco Basin, *Crit. Quat. Stratigr.*, *25*(23–24), 3216–3227, doi:10.1016/j.quascirev.2006.03.014.

Hughen, K. A., J. R. Southon, S. J. Lehman, and J. T. Overpeck (2000), Synchronous radiocarbon and climate shifts during the last deglaciation, *Science*, *290*(5498), 1951, doi:10.1126/science.290.5498.1951.

Hughen, K. A., J. R. Southon, C. J. H. Bertrand, B. Frantz, and P. Zermeño (2004), Cariaco Basin calibration update: Revisions to calendar and ^{14}C chronologies for Core Pl07-58Pc, *Radiocarbon*, *46*(03), 1161–1187, doi:10.1017/S0033822200033075.

Jayne, S. R., L. C. S. Laurent, and S. T. Gille (2004), Connections between ocean bottom topography and Earth's climate, *Oceanography*, *17*, 65–74, doi:10.5670/oceanog.2004.68.

Key, R. M., A. Kozyr, C. L. Sabine, K. Lee, R. Wanninkhof, J. L. Bullister, R. A. Feely, F. J. Millero, C. Mordy, and T.-H. Peng (2004), A global ocean carbon climatology: Results from Global Data Analysis Project (GLODAP), *Global Biogeochem. Cycles*, *18*, GB4031, doi:10.1029/2004GB002247.

Köhler, P., R. Muscheler, and H. Fischer (2006), A model-based interpretation of low-frequency changes in the carbon cycle during the last 120,000 years and its implications for the reconstruction of atmospheric Δ^{14}C, *Geochem. Geophys. Geosyst.*, *7*, Q11N06, doi:10.1029/2005GC001228.

Laj, C., H. Guillou, and C. Kissel (2014), Dynamics of the earth magnetic field in the 10–75 kyr period comprising the Laschamp and Mono Lake excursions: New results from the French Chaîne des Puys in a global perspective, *Earth Planet. Sci. Lett.*, *387*, 184–197, doi:10.1016/j.epsl.2013.11.031.

Lohmann, G. (1998), The influence of a near-bottom transport parameterization on the sensitivity of the thermohaline circulation, *J. Phys. Oceanogr.*, *28*(10), 2095–2103, doi:10.1175/1520-0485(1998)028<2095:TIOANB>2.0.CO;2.

Lohmann, G., and S. Lorenz (2000), On the hydrological cycle under paleoclimatic conditions as derived from AGCM simulations, *J. Geophys. Res.*, *105*(D13), 17,417–17,436, doi:10.1029/2000JD900189.

Maier-Reimer, E., U. Mikolajewicz, and K. Hasselmann (1993), Mean circulation of the Hamburg LSG OGCM and its sensitivity to the thermohaline surface forcing, *J. Phys. Oceanogr.*, *23*(4), 731–757, doi:10.1175/1520-0485(1993)023<0731:MCOTHL>2.0.CO;2.

Paul, A., and C. Schäfer-Neth (2003), Modeling the water masses of the Atlantic Ocean at the Last Glacial Maximum, *Paleoceanography*, *18*(3), 1058, doi:10.1029/2002PA000783.

Peterson, L. C., J. T. Overpeck, N. G. Kipp, and J. Imbrie (1991), A high-resolution late Quaternary upwelling record from the anoxic Cariaco Basin, Venezuela, *Paleoceanography*, *6*(1), 99–119, doi:10.1029/90PA02497.

Prange, M., G. Lohmann, and A. Paul (2003), Influence of vertical mixing on the thermohaline hysteresis: Analyses of an OGCM, *J. Phys. Oceanogr.*, *33*(8), 1707–1721, doi:10.1175/2389.1.

Prange, M., G. Lohmann, V. Romanova, and M. Butzin (2004), Modelling tempo-spatial signatures of Heinrich events: Influence of the climatic background state, *Quat. Sci. Rev.*, *23*(5–6), 521–527, doi:10.1016/j.quascirev.2003.11.004.

Reimer, P. J., et al. (2013), IntCal13 and Marine13 radioacarbon age calibration curves 0–50,000 years cal BP, *Radiocarbon*, *55*, 1869–1887, doi:10.2458/azu_js_rc.55.16947.

Ritz, S. P., T. F. Stocker, and S. A. Müller (2008), Modeling the effect of abrupt ocean circulation change on marine reservoir age, *Earth Planet. Sci. Lett.*, *268*(1–2), 202–211, doi:10.1016/j.epsl.2008.01.024.

Sarnthein, M., K. Winn, S. J. A. Jung, J.-C. Duplessy, L. Labeyrie, H. Erlenkeuser, and G. Ganssen (1994), Changes in East Atlantic Deepwater circulation over the last 30,000 years: Eight time slice reconstructions, *Paleoceanography*, *9*(2), 209–267, doi:10.1029/93PA03301.

Sarnthein, M., R. Gersonde, S. Niebler, U. Pflaumann, R. Spielhagen, J. Thiede, G. Wefer, and M. Weinelt (2003), Overview of Glacial Atlantic Ocean Mapping (GLAMAP 2000), *Paleoceanography*, *18*(2), 1030, doi:10.1029/2002PA000769.

Sarnthein, M., S. Balmer, P. M. Grootes, and M. Mudelsee (2015), Planktic and benthic ^{14}C reservoir ages for three ocean basins, calibrated by a suite of ^{14}C plateaus in the glacial-to-deglacial Suigetsu atmospheric ^{14}C record, *Radiocarbon*, *57*(1), 129–151, doi:10.2458/azu_rc.57.17916.

Schäfer-Neth, C., and A. Paul (2001), Circulation of the glacial Atlantic: A synthesis of global and regional modeling, in *The Northern North Atlantic: A Changing Environment*, edited by P. Schäfer et al., pp. 441–462, Springer, Berlin.

Sikes, E. L., and T. P. Guilderson (2016), Southwest Pacific Ocean surface reservoir ages since the last glaciation: Circulation insights from multiple-core studies, *Paleoceanography*, *31*, 298–310, doi:10.1002/2015PA002855.

Singarayer, J. S., D. A. Richards, A. Ridgwell, P. J. Valdes, W. E. N. Austin, and J. W. Beck (2008), An oceanic origin for the increase of atmospheric radiocarbon during the Younger Dryas, *Geophys. Res. Lett.*, *35*, L14707, doi:10.1029/2008GL034074.

Skinner, L. C., F. Primeau, E. Freeman, M. de la Fuente, P. A. Goodwin, J. Gottschalk, E. Huang, I. N. McCave, T. L. Noble, and A. E. Scrivner (2017), Radiocarbon constraints on the glacial ocean circulation and its impact on atmospheric CO_2, *Nat. Commun.*, *8*, 16010, doi:10.1038/ncomms16010.

Southon, J., A. L. Noronha, H. Cheng, R. L. Edwards, and Y. Wang (2012), A high-resolution record of atmospheric ^{14}C based on Hulu cave speleothem H82, *Quat. Sci. Rev.*, *33*, 32–41, doi:10.1016/j.quascirev.2011.11.022.

Stern, J. V., and L. E. Lisiecki (2013), North Atlantic circulation and reservoir age changes over the past 41,000 years, *Geophys. Res. Lett.*, *40*, 3693–3697, doi:10.1002/grl.50679.

Sweeney, C., E. Gloor, A. R. Jacobson, R. M. Key, G. McKinley, J. L. Sarmiento, and R. Wanninkhof (2007), Constraining global air-sea gas exchange for CO_2 with recent bomb ^{14}C measurements, *Global Biogeochem. Cycles*, *21*, GB2015, doi:10.1029/2006GB002784.

Thornalley, D. J. R., S. Barker, W. S. Broecker, H. Elderfield, and I. N. McCave (2011), The deglacial evolution of North Atlantic deep convection, *Science*, *331*(6014), 202–205, doi:10.1126/science.1196812.

Thornalley, D. J. R., H. A. Bauch, G. Gebbie, W. Guo, M. Ziegler, S. M. Bernasconi, S. Barker, L. C. Skinner, and J. Yu (2015), A warm and poorly ventilated deep Arctic Mediterranean during the last glacial period, *Science*, *349*(6249), 706–710, doi:10.1126/science.aaa9554.

Toggweiler, J. R., K. Dixon, and K. Bryan (1989), Simulations of radiocarbon in a coarse-resolution world ocean model: 1. Steady state pre-bomb distributions, *J. Geophys. Res.*, *94*(C6), 8217–8242, doi:10.1029/JC094iC06p08217.

Marine Radiocarbon Reservoir Age Simulations for the Past 50,000 Years
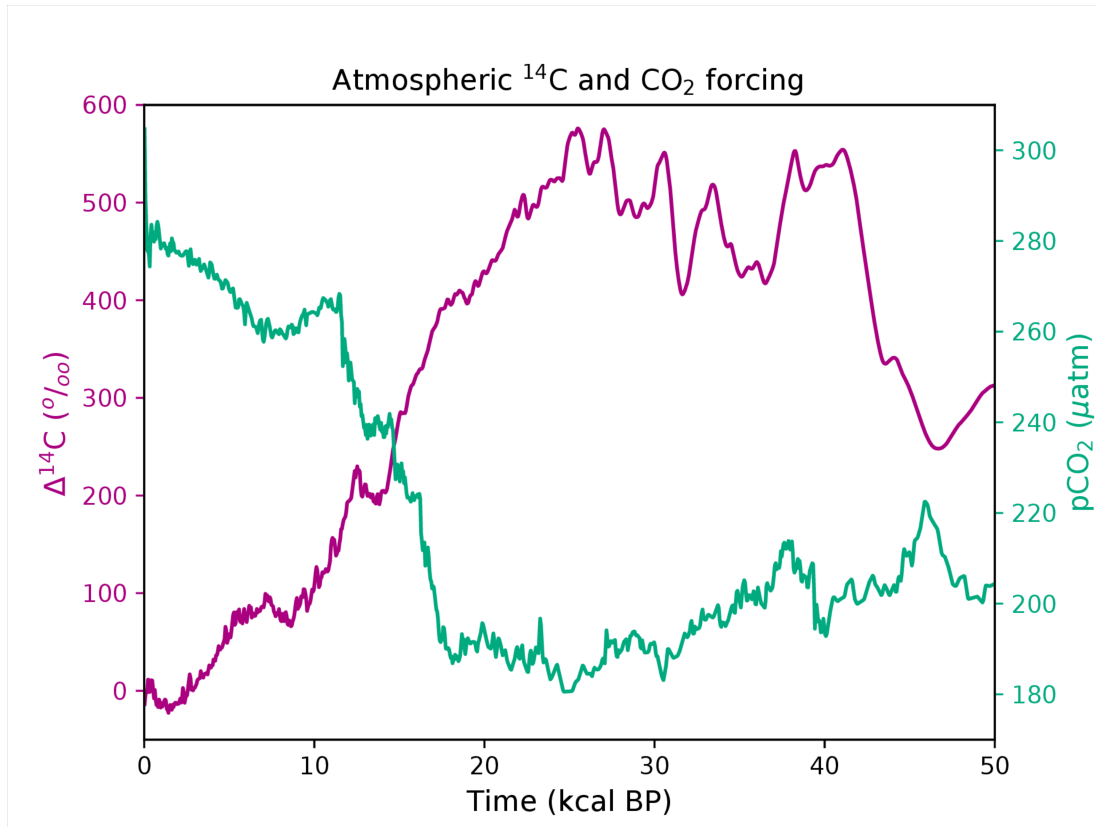
M. Butzin[1], P. Köhler[1], and G. Lohmann[1]

[1]Alfred-Wegener-Institut Helmholtz-Zentrum für Polar-und Meeresforschung (AWI), Bremerhaven, Germany

Contents of this file

Introduction

The supporting figure shows reconstructed curves of atmospheric radiocarbon ($\Delta^{14}C$) and carbon dioxide (pCO_2) used as boundary conditions in our simulations.

Figure S1. Histories of atmospheric Δ^{14}C according to IntCal13 [*Reimer et al.*, 2013] and pCO$_2$ (based on mixing ratios reconstructed by *Bereiter et al.* [2015].

References

Bereiter, B., S. Eggleston, J. Schmitt, C. Nehrbass-Ahles, T. F. Stocker, H. Fischer, S. Kipfstuhl, and J. Chappellaz (2015), Revision of the EPICA Dome C CO$_2$ record from 800 to 600 kyr before present, *Geophys. Res. Lett.*, *42*(2), 542–549, doi:10.1002/2014GL061957.

Reimer, P. J. et al. (2013), IntCal13 and Marine13 radioacarbon age calibration curves 0–50,000 years cal BP, *Radiocarbon*, *55*, 1869–1887, doi:10.2458/azu_js_rc.55.16947.